Journal of Thermal Analysis and Calorimetry, Vol. 78 (2004) 865–884

THE EFFECT OF CHAIN EXTENSION ON THE THERMAL BEHAVIOUR AND CRYSTALLINITY OF REACTIVE EXTRUDED RECYCLED PET

F. Awaja[1], *F. Daver*[1*], *E. Kosior*[2] *and F. Cser*[3]

[1]School of Aerospace, Mechanical and Manufacturing Engineering, RMIT University, PO Box 71, Bundoora, Victoria 3083, Australia
[2]Visy Technical Centre, 23 Ash Road, Prestons, NSW 2170, Australia
[3]Rheology and Materials Processing Centre, RMIT University, GPO Box 2476V, Melbourne, Victoria 3001, Australia

Abstract

Recycled poly(ethylene terephthalate) (R-PET) was chain extended with pyromellitic dianhydride (PMDA) in a commercial size twin-screw reactive extrusion system. Temperature-modulated differential scanning calorimetry (TMDSC) was used to evaluate the effect of the chain extension process on the thermal transitions and crystallinity of R-PET. Reactive extruded recycled PET (RER-PET) samples were tested based on different PMDA concentration and reactive extrusion residence times. The glass transition temperature (T_g) did not show a significant change as a function of PMDA addition or the extrusion residence time. Melting temperature (T_m) and crystallisation temperature (T_c) decreased with increasing PMDA concentration and with increasing extrusion residence time. RER-PET samples showed double melting peaks, it is believed that different melting mechanism is the reason behind this phenomenon. The crystallinity of RER-PET samples is lower than that of R-PET. RER-PET samples at constant PMDA concentration showed a decrease in crystallinity with increasing extrusion residence time. Results suggest that the reactive extrusion process is more dependent on PMDA concentration rather than reactive extrusion process residence time.

Keywords: chain extension, crystallinity, reactive extrusion, recycled PET, TMDSC

Introduction

Poly(ethylene terephthalate) (PET) is a widely used thermoplastic polyester in manufacturing of textile fibers, soft-drink bottles, photographic films, audio/video tapes and packaging films. Owing to the increased awareness of environmental issues, recycling of PET has recently attracted great interest around the world. However, the use of recycled PET (R-PET) in many value-added applications is limited due to lack of desirable mechanical properties and high melt strength, which depend on the molecular characteristics, such as average molecular mass, molecular mass distribution and chain branching. During the melt processing of R-PET at high temperatures, R-PET under-

* Author for correspondence: E-mail: daver@rmit.edu.au

1388–6150/2004/ $ 20.00

Akadémiai Kiadó, Budapest
Kluwer Academic Publishers, Dordrecht

goes a series of thermal and hydrolytic degradation reactions in the presence of water and contaminants, such as adhesives, poly(vinyl chloride) (PVC), etc. [1]. This leads to the decrease in intrinsic viscosity ([η]) by formation of low molecular mass PET with a significant increase of carboxyl and hydroxyl end groups [2]. To overcome this problem, chain extenders have been employed, and chain extension process has been successfully used in increasing the molecular mass, intrinsic viscosity and melt strength during melt processing of R-PET [3–7]. PET chain extension is a process in which a di- or poly-functional low molecular mass material is reacting with PET carboxyl or hydroxyl end groups to rejoin the broken chains that are the results of PET chain scissions. The chain extenders are generally poly-functional, thermally stable and easily available, and have the capability of fast reaction with PET end groups without undesirable by-products. Some of the extenders reported in the literature are di- and multi-functional epoxies [6–10], diisocyanates [7], dianhydrides [11] and bis-oxazolines [1, 3, 7, 12]. The chain extender, pyromellitic dianhydride (PMDA) has been chosen by many researchers [4, 13–16] for the PET chain extension process due to its fast reaction rate with PET, tetra functionality, thermal stability and low cost.

Chain extended R-PET usually exhibits higher molecular mass and intrinsic viscosity than R-PET, and it also has less chain flexibility and denser molecular structure. The increase in molecular mass of chain extended R-PET will alter the crystallisation rate and the crystallinity level, and that will indeed influence R-PET performance and properties including thermal transitions, such as glass transition temperature (T_g), melting temperature (T_m) and crystallisation temperature (T_c) [4, 5, 7].

There have been rigorous efforts by many researchers to understand the effects of chain extension process on thermal transitions of virgin PET [8, 9, 17–19]. Using differential scanning calorimetry (DSC), the decrease in T_g, T_c, T_m and crystallinity values is observed after virgin PET has been chain extended by different chain extenders. Haralabakopoulos *et al.* [8] reported a decrease in PET thermal transition values with increasing diepoxides chain extender concentration and reaction time. Bikiaris and Karayannidis [9] noticed a decrease in T_m while there was no significant change in T_g when virgin PET had been chain extended by diepoxides. Nevertheless, Inata and Matsumura [17] reported that virgin PET chain extension process did not have a serious effect on T_m values. In these results mentioned above, various chain extenders have been used with different chain extender concentrations, and this explains the degree of significance of chain extension process on thermal transitions of virgin PET. It is generally expected that the increases in molecular mass and η decrease the T_c and T_m values.

Crystallinity of PET strongly affects the end-use application, and this mainly depends on the molecular structure and crystallisation conditions [20]. The decrease in the crystallinity is expected during chain extension process due to a high degree of branching and chain entanglements [4]. However, crystallisation at high temperatures increases the crystallinity due to the ease of chain disentanglement [18]. In a recent study, by Torres *et al.* [2], it was mentioned that the impurities present in the R-PET after the chain extension could act as nucleating agents promoting crystallisation. Furthermore, Rosu *et al.* [21] have reported that addition of a branched PET to a linear

PET also increases its crystallinity. This is particularly important to the current study as PET chain extension process with tetra functional PMDA is known to introduce substantial branching structures. It has been found in our previous study that the degree of branching primarily depends on the PMDA concentration [22].

In this study, temperature modulated differential scanning calorimetry (TMDSC) was used to investigate the effect of the chain extension process of R-PET on thermal behaviour and crystallinity of the RER-PET. TMDSC thermal analysis has been widely used to study the first order transitions such as melting and crystallinity [23–25]. The chain extension of R-PET by reactive extrusion was performed using an industrial scale PET extruder with PMDA as the chain extender. The PMDA concentrations and extruder parameters were varied in order to produce materials suitable for injection stretch blow moulding. TMDSC has been proven to be more powerful than the conventional DSC [26, 27], also its theory and operating principles are extensively described in [28, 29]. TMDSC gives accurate heat capacity measurements and separates reversible and irreversible phenomena, and it has better resolution and sensitivity. The independent measurement of the total heat flow and the heat capacity makes it possible to divide the heat flow into two kinds of processes: reversing and non-reversing (kinetic) heat flows respectively. The separation of these two components allows the study of thermal transitions in more detail. TMDSC has been used for the analysis of the melting of virgin PET [30–33]. The aim of this study is to provide an insight on the changes of thermal transitions and crystallinity of reactive extruded R-PET (RER-PET) using the TMDSC technique.

Experimental

Reactive extrusion

Since the chain extension process was more convenient when it was performed in an existing R-PET extrusion facility, the reactive extrusion process experiments were implemented on a PET commercial size co-rotating twin-screw extruder (L/D=33, D=70 mm) with a maximum capacity of 500 kg h^{-1}. The extruder was operated under vacuum so that all light components resulting from the degradation reactions were forced out continuously. The processing variables examined were PMDA chain extender concentration and extruder process residence time. PMDA concentrations investigated were 0.05, 0.08, 0.1, 0.15, 0.2, 0.25 and 0.3 mass% at a constant extruder residence time of 45 s which is taken as the unit relative residence time of 1. Extruder flow rates equivalent to 1.11, 1.25, 1.43, 2 and 3 relative residence times, at a constant PMDA concentration of 0.15 mass%, were also investigated. Flakes of R-PET ($[\eta]$=0.675 dL g^{-1}) processed at Visy Industries Pty Ltd., Australia, from post-consumer bottles were subjected to intensive drying at 170°C before feeding to the extruder. PMDA (99.7%) was obtained from Nippon Shokubai Co. Ltd., Japan. PMDA was directly fed to the feeding section of the extrusion line as a powder via volumetric feeder. Extrudate was cooled in water at 20°C, dried by a stream of hot air at 170°C and cut into pellets. The details of operation conditions are reported elsewhere [22].

Intrinsic viscosity [η]

Intrinsic viscosity measurements of R-PET, RER-PET and virgin PET ([η]=0.8 dL g^{-1}, M_n=31505.5 g mol^{-1}, supplied by Eastman chemical company, USA) samples were performed using AMV 200 rolling ball viscometer. A mixture of 60:40 (by mass) phenol and 1,1,2,2-tetrachloroethane at 120ºC was used to dissolve the PET samples. Solutions of PET were tested at a PET concentration of 0.5% at 25°C.

The apparent number average molecular mass (M_n) for all samples were calculated according to the Mark–Houwink equation, $[\eta]=k M_n^a$, where k and a are constants, and for PET they are equal to $2.75 \cdot 10^{-4}$ dL g^{-1} and 0.77, respectively [34].

Temperature modulated differential scanning calorimetry (TMDSC)

All thermal measurements and treatments were done on a Thermal Analyst 2920 system from TA instrument Inc. with TMDSC. Helium gas with a flow rate of 30 mL min^{-1} was purged through the DSC cell. A refrigerating cooling system was used with a flow rate of 100 mL min^{-1} of nitrogen. The instrument was calibrated for the temperature using water and indium at a heating and cooling scanning rates of 2°C min^{-1}. The heat flow was calibrated with heat of fusion of indium, the heat capacity constant was calibrated with the heat capacity of sapphire using p=40 s modulation period and A_t=0.6°C modulation amplitude. The instrument was calibrated according to the requirements and a full detailed description was given in [35]. Specimens (8–12 mg) were cut as flat slices to avoid the effects of heat transfer as far as possible and the specimen were encapsulated in the aluminium pans. Two consecutive heating and cooling runs were employed using 2°C min^{-1} heating and cooling rates respectively in both runs. A sinusoidal modulation with a period of 40 s, temperature amplitude of 0.6°C was used from 20 to 290°C temperature limits. This is a medium depth type of modulation with slight cooling during the heating [35]. The first heating and cooling runs served to eliminate the thermal history of the material. The second heating and cooling runs served as analytical runs where the peak melting temperature (T_m) and enthalpy of melting (ΔH_m) were obtained from the total heat flow curves and glass transition temperature (T_g) from the heat capacity curves. T_g again was obtained from the heat capacity curve, while peak crystallisation temperature (T_c) and enthalpy of crystallisation (ΔH_c) were taken from the total heat flow curves recorded during the cooling run. The cold crystallisation temperature (T_{cc}) and enthalpy of cold crystallisation (ΔH_{cc}) were obtained from the first heating run. The enthalpies of fusion and crystallisation were integrated from the total heat flow curves using lower integration limits of 110°C and upper integration limits as the end of the melting process as well as the start of the crystallisation process. Glass transition temperatures were obtained as the inflexion point of the heat capacity curves at the transition.

The modulated DSC experiments normally show four types of curves. The total heat flow curve (same as conventional DSC curve) is obtained as an average of the modulated heat flow values, the heat capacity is obtained as the main amplitude of the oscillation of the response heat flow curve. These are the primary measured curves obtained by Fourier transformation of the oscillating heat flow curve as the

function of the oscillating temperature function. The heat capacity curve is multiplied by the actual underlying heating rate and so an in-phase curve (reversing or storage) heat flow curve is obtained while out-of-phase curve (loss or kinetic, or non-reversing, NR) heat flow curve is derived by subtracting the reversing heat flow values from those of the total heat flow [36]. The reversing heat flow is supposed to represent reversible transition processes and the NR heat flow is particularly useful for determining irreversible processes such as annealing or crystallisation during melting. The standard deviation of transition enthalpies in this instrument is 3% or better in case of well developed single transition peaks [35].

Twelve different reactive extrusion experimental samples were tested. Virgin PET and R-PET samples were also tested for comparison reasons. Total crystallinity of the samples was calculated from the enthalpy of total heat flow endotherms taken from 110°C to the last crystal disappearing temperature (265°C). The heat of fusion for the perfect crystals is taken as 135 J g^{-1} [12].

Results and discussion

Reactive extrusion process of R-PET with PMDA was successfully implemented as it is seen from the data in Table 1. The M_n and [η] values, which give a measure of effectiveness of coupling and/or branching reactions of R-PET (Fig. 1), have increased with increasing PMDA concentration and extruder residence time. However, the reactive extrusion process has limits for the PMDA concentration and extruder residence times examined. Full description of the reactive extrusion process and the PET-PMDA chain extension reaction mechanisms are presented in our previous paper [22]. In our previous study, we have found three different reactions between R-PET and PMDA depending on the PMDA concentration. Those reactions are coupling, branching and complex branching or cross-linking. As seen in Fig. 1, coupling reaction takes place when one molecule of PMDA joins two R-PET chains. Branching reaction takes place when PMDA molecule joins more than two R-PET chains. Complex branching reactions undergo when more than one PMDA molecule joins more than two R-PET degraded chains. The results of the cross-linking test showed that there was not a significant amount of gel (less than 4%), which was produced because of PET-PMDA reaction at different PMDA concentrations [22]. In other words, branching reactions at such PMDA concentrations did not reached the point of heavy cross-linking or gel formation.

TMDSC curves of R-PET with various PMDA concentrations

Figure 2 shows the total heat flow curves for a RER-PET sample with 0.15% of PDMA and a relative residence time of 1.25 as an example. Both heating and cooling runs are shown in Fig. 2. The first heating run has a strong step at the glass transition temperature, then a cold crystallisation process is followed. The melting peak contains one broad peak with a single peak melting temperature at 250°C range. The slow cooling results in crystallisation of the PET samples therefore there is no cold

Table 1 The intrinsic viscosity [η] and number average apparent molecular mass (M_n) of RER-PET samples at a – different PMDA concentration with constant extrusion flow rate and b – different reactive extruder flow rates with constant PMDA concentration

a – extrusion flow rate: 500 kg h^{-1}

PMDA/%	[η]/dL g^{-1}	M_n/g mol^{-1}
0.00	0.675	29211
0.05	0.709	30958
0.08	0.712	31320
0.10	0.720	31800
0.15	0.728	32165
0.20	0.731	32470
0.25	0.768	34495
0.30	0.817	37813

b – PMDA concentration: 0.15%

Flow rate/kg h^{-1}	[η]/dL g^{-1}	M_n/g mol^{-1}
200	0.800	36740
250	0.780	35487
350	0.763	34680
400	0.758	34123
450	0.730	32408
500	0.728	32165

crystallisation on the curve and parallel the glass transition temperature is increased with respect to the completely amorphous material of the first heating run. The most interesting change can be found in the melting peak what turns to be doubled. The highest peak is with lower peak temperature marked by 'A'. The second peak marked by 'B' is at nearly the same temperature as the melting peak of the first heating run.

Figure 3 compares the different components of the second heating processes. It is obvious from this comparison, the melting process marked by 'A' dominates the reversing heat flow and the second melting process marked by 'B' appears only as a shoulder. Non-reversing heat flow shows both peaks separated. This kind of behaviour was found at all of the samples.

Figure 4 compares the total heat flow curves of RER-PET samples obtained at different PMDA concentrations, after crystallising at 2°C min^{-1} rate, while Fig. 5 shows the corresponding heat capacity curves. Only two thermal transitions, glass transition and melting can clearly be recognised from all curves. The T_g inflection was seen as a step change in the heat capacity curves and also in the total heat flow curves. In some cases a small endothermic peak is seen in the total and in the NR heat flow curves during the first heating runs. This endothermic peak can be found at the higher tempera-

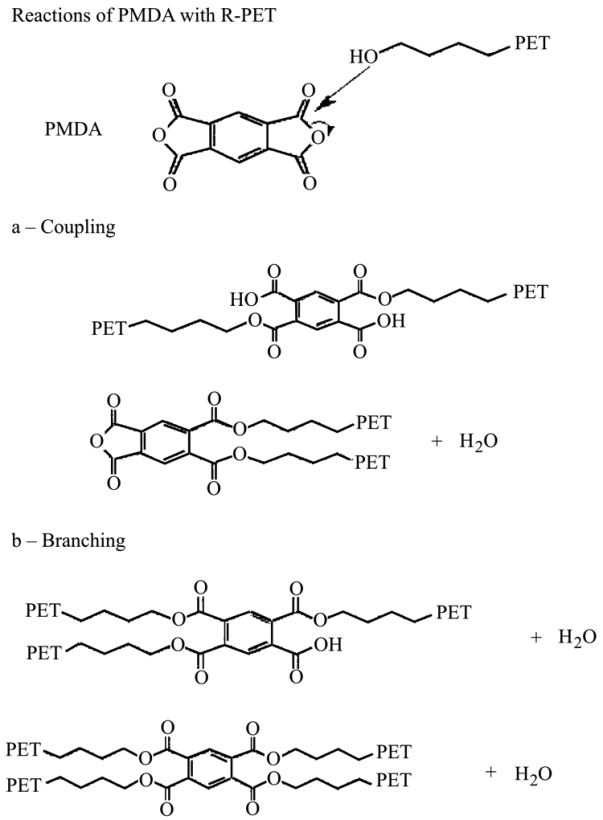

Fig. 1 Reactions of PMDA with PET

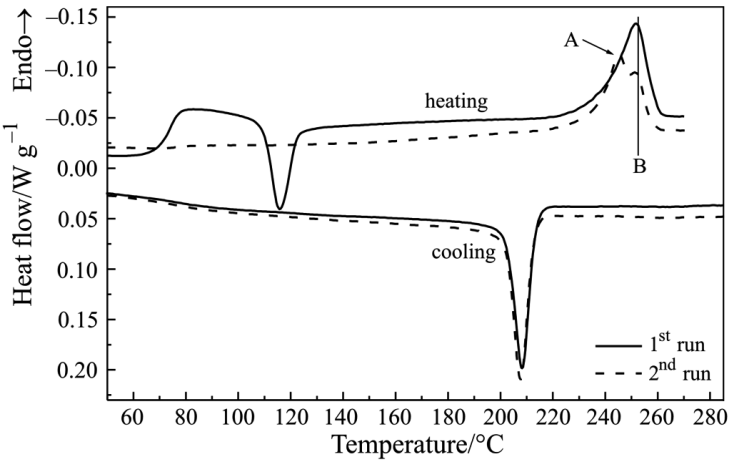

Fig. 2 TMDSC total heat flow curves of a modified RER-PET sample obtained at 0.15% PMDA concentrations at a relative residence time of 1.25. Two heating and cooling cycles, respectively, are included for comparison

ture end of the glass transition. It is called enthalpy relaxation peak, produced by aging of the polymer is usually obscured in the conventional DSC curve [29].

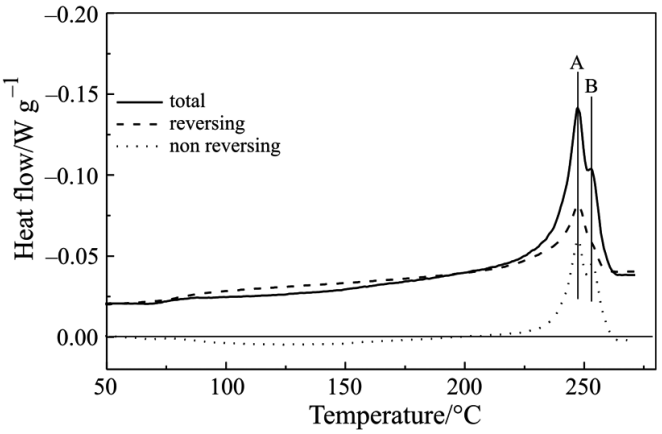

Fig. 3 The comparison of the total heat flow, the reversing heat flow and the non-reversing heat flow curves of the second heating cycle of sample with 0.15% of PDMA and a relative residence time of 1.43

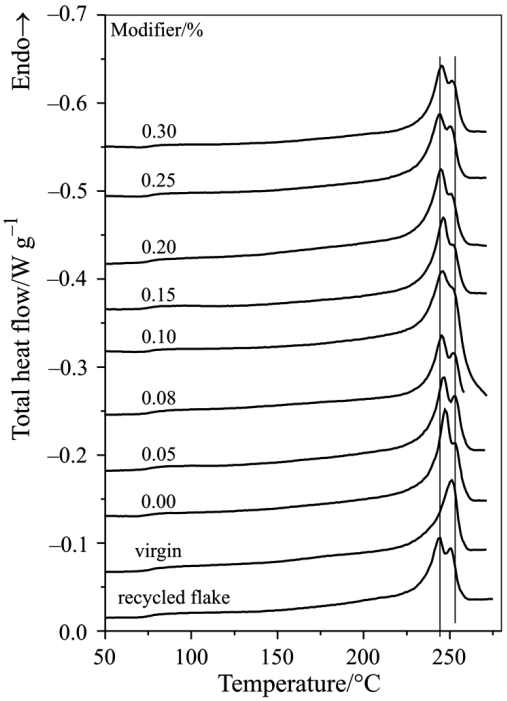

Fig. 4 TMDSC total heat flow curves of RER-PET samples obtained at different PDMA content. Recycled and virgin PET curves are included for comparison

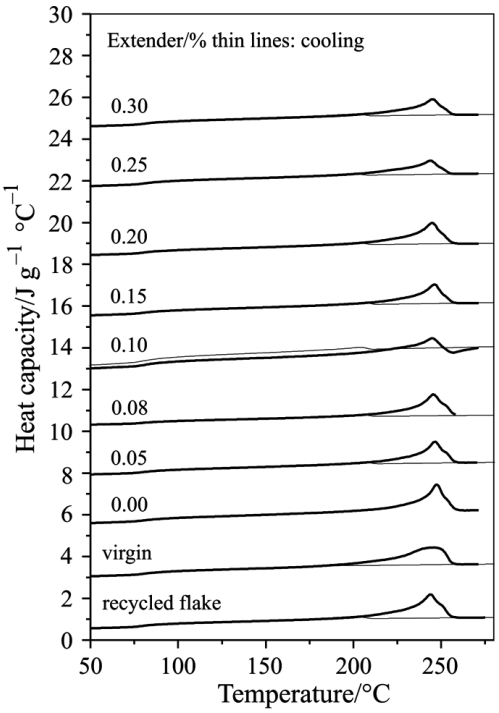

Fig. 5 TMDSC heat capacity curves of RER-PET samples obtained at different PDMA content. Recycled and virgin PET curves are included for comparison

The melting transition can be seen in both sets of curves. It was seen that RER-PET samples revealed a double melting peak during the MDSC heating run and RER-PET samples have about 6–8°C difference between the low-temperature (A, T_{m1}), and the high-temperature melting peak (B, T_{m2}). The double or multiple melting behaviour is not uncommon for PET and modified PET materials depending on the crystallisation conditions and it has not been well understood to date [20, 37]. The multiple melting peak behaviour of semi-crystalline polymers crystallised from the melt has been investigated extensively and it is proposed to link to partial melting and re-crystallisation and remelting (mrr), to distribution of crystals with different lamellar thickness, and to melting of different crystal structures [35]. As the crystals start to melt, the partially melted disentangled chains would promote local re-crystallisation resulting in secondary crystals, which melt at a higher temperature. In contrast, the slow cooling treatment allows enough time for segregation of the fractions with different degrees of branching to form two distinct morphologies resulting in the double peaks. In the case of isothermally crystallised PET, it is suggested that the double melting behaviour is associated with the mrr process [20]. Nevertheless, it is generally not possible to detect the recrystallisation exotherm in the conventional DSC scan due to its superposition to the melting endotherm.

As mentioned previously, the reversing heat flow component contains the reversible component of the total heat flow, while the NR component represents all irreversible component of the total heat flow at the time and temperature of the modulation. In TMDSC curves, the endothermic contributions (e.g. melting) can be seen in both reversing and NR components, whereas exothermic transitions (e.g. recrystallisation, crystal annealing and perfection) are only appeared in the NR curve [39–41]. Therefore, it is possible to distinguish endothermic and exothermic contributions by examining the reversing and NR heat flow curves. The curves displayed in Fig. 4 show only broad, double melting endothermic peaks, and no exothermic activity due to the annealing and/or re-crystallisation was detected in the NR heat flow curves before and during the melting. Therefore, the double melting peaks appearing in the TMDSC curves may not be attributed to the mrr process. Tan *et al*. [37] have recently claimed that the double melting peaks of isothermally crystallised PET are associated with two distinct crystal populations with different lamellar thicknesses. Nonetheless, a double melting reversing endothermic peak, in conjunction with a recrystallisation exothermic non-reversing contribution has been observed for isothermally crystallised PET [39], syndiotactic polystyrene [41] and polyethylenes [42]. It has also been observed at polypropylene (PP) and there was no exothermic recrystallisation detected there [43]. In both at PP and here at PET the two peaks found in total heat flow curve have different peak heights in the reversing and in the NR heat flow curves respectively. The peak with lower peak temperature has much higher height in reversing heat flow than that of the second peak, but this is reversed in the NR heat flow curves. The two peaks observed at PP were influenced by adding LLDPE to PP. The peak with lower peak temperature was increased and the second peak with higher peak temperature was decreased by increasing amount of LLDPE [43]. This suggests that the melting peak at lower peak temperature has different melting mechanism than the second melting peak. The former represents the dissolution of PET crystals within the liquid amorphous material which exhibits to be a solvent with respect to the PET. The second peak corresponds to the traditional collapsing mechanism of the polymer crystals.

Moreover, it was observed that the TMDSC curves obtained under the same condition for RER-PET samples but with extrusion history (not shown here), i.e., quenched cooling, showed only a sharp single melting peak. The rapidly cooled PET material is generally metastable, it is a supercooled, a frozen liquid and it experiences recrystallisation during heating. The heating rate used was 2°C min^{-1}, which is regarded as a relatively slow rate, and at that rate PET molecules would have enough time to undergo recrystallisation. However, no recrystallisation and annealing exotherm of these samples was detected during the second heating scan. In comparison, R-PET also demonstrates a double melting peak while virgin PET has a single sharp melting peak, as it is shown in Fig. 4. The single melting peak of virgin PET is indicative of homogeneity of the structure. The homogeneous crystallisation is also confirmed by the total heat flow curves recorded during the cooling runs as shown in Fig. 6.

The area under the crystallisation exotherm measures the amount of primary crystallinity. The decrease in ΔH_c values (Table 2) on the addition of PMDA suggests reduced crystallinity due to the chain extension. Entangled chains have reduced mobil-

Table 2 The thermal characteristics of RER-PET, R-PET and virgin PET. Temperatures are in °C and enthalpies are in J g^{-1}

PMDA/%	[a]T_{cc}	[a]ΔH_{cc}	ΔH_c	[b]T_{m1}	[b]T_{m2}	[c]$\Delta H_{m,R}$	[c]$\Delta H_{m,NR}$	[c]$\Delta H_{m,total}$
0.00	113.8	28.8	47.5	247.2	254.1	44.2	17.2	62.0
0.05	–	–	50.3	246.5	253.8	25.3	28.8	54.2
0.08	–	–	46.9	245.5	253.3	21.4	27.7	49.1
0.10	–	–	41.9	245.0	253.2	25.4	25.9	51.4
0.15	115.6	31.1	49.9	246.1	253.4	21.2	32.6	53.7
0.20	115.5	26.1	47.6	246.3	252.8	23.2	28.0	51.2
0.25	115.9	27.3	47.7	244.6	251.9	27.1	35.3	62.4
0.30	115.1	26.0	45.5	247.9	250.8	31.3	16.3	47.6
Relative residence time								
1.00	115.6	31.1	79.4	245.8	253.1	21.2	32.6	53.7
1.11	113.1	24.8	46.2	246.5	253.6	24.8	24.3	49.1
1.25	115.7	25.8	51.3	245.2	252.3	31.3	13.5	44.8
1.43	116.5	25.7	44.0	245.1	252.6	27.6	38.6	66.1
2.00	116.6	27.1	46.8	245.7	252.8	27.7	35.7	63.4
2.50	118.6	24.1	47.8	244.4	252.0	24.3	28.3	52.6

[a]Values were obtained from the first heating curve.
[b]Melting temperature values of total heat flow curves are reported.
[c]R=reversing, NR=non-reversing and total=total heat flow curve

ity in the liquid phase, and that leads to difficulties for the chains to be organised in the crystalline structure. The chain entanglements are eased with increasing temperature and result in some of the lower molecular mass chains able to be fully or partially organised in the crystalline structure. However, the chain entanglement effect is not fully overcome by the high temperature, as indicated by the decrease of the crystallinity when PMDA is increased as shown in Fig. 7.

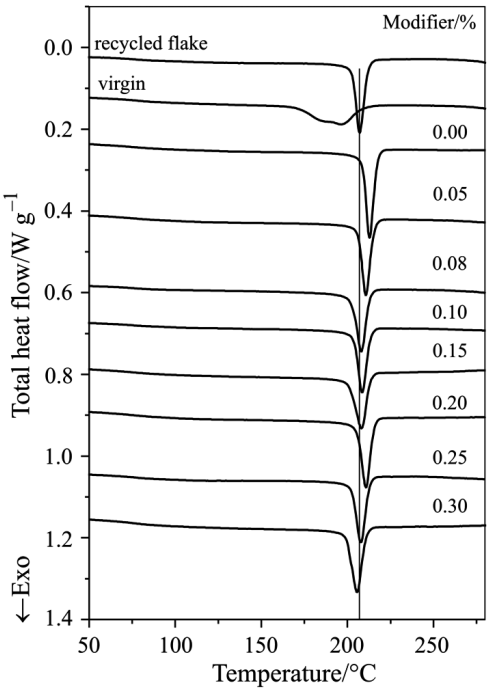

Fig. 6 TMDSC total heat flow curves of RER-PET samples at different PDMA content upon cooling. Recycled and virgin PET curves are included for comparison

In general, amorphous PET can be crystallised over the broad range between T_g and melting. Cold crystallisation peak (Table 2), which is common for the highly amorphous PET was only observed in the samples of extrusion history. Thus, by quenching RER-PET melt samples after the extrusion, a glassy, amorphous polymer was obtained. Semi-crystalline PET was then obtained by slow crystallisation at a 2°C min^{-1} rate from the melt.

The enthalpies obtained from the total heat flow curves of both first and second heating runs are shown in Fig. 7. Those of reversing and NR components obtained in the second heating runs are shown in Table 2. The scattering of the data is high. If we disregard sample with PMDA content of 0.25 mass%, a decrease in the total melting enthalpy can be observed. As the PMDA concentration was increased, the reversing contribution increased and the non-reversing contribution decreased. In RER-PET

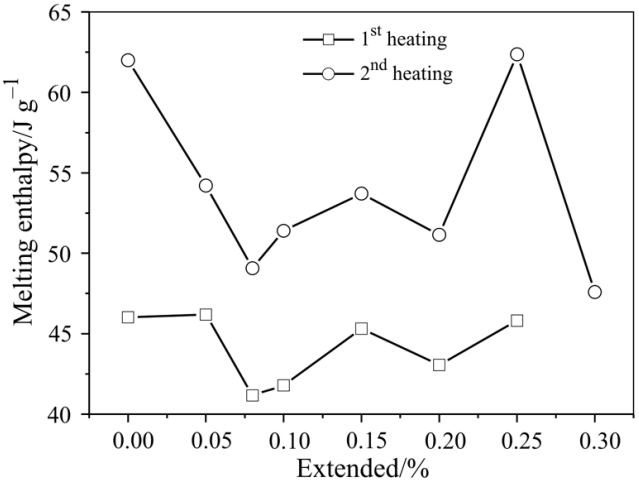

Fig. 7 Enthalpies of the melting and crystallization of RER-PET as a function of the PDMA content

samples, the reversing component was smaller than the NR component, except for the RER-PET sample prepared at 0 and at 0.3 mass% PMDA concentration. This suggested again a solution mechanism of melting, since the more branched the structure the higher the solution effect observed. Table 2 also shows the enthalpies of crystallisation. These values are close to those observed in total melting enthalpies of the first heating runs.

The nature of chain structure and chain entanglements of R-PET was significantly changed during the chain extension process. The fact that PMDA has the ability to react tetra functionally with PET chains is a decisive factor in promoting coupling and branching reactions, and therefore, chains extension leads to a different molecular structure and architecture [4]. The increased branching and chain entanglements are of great importance to the change in melting and crystallisation behaviour of RER-PET. The chain entanglement, looping of one chain around another, generally occurs in linear PET with high molecular masses. The relaxation of chain entanglements greatly depends on the temperature, and it is a very slow process.

Variations of T_g, T_m, T_c and crystallinity with PMDA concentration

The variations of T_g, T_m, T_c values and crystallinity with PMDA concentration are displayed in Figs 8 and 9. Figure 8 illustrates that the peak melting temperatures as well as the crystallisation peak temperatures generally decrease by increased PDMA content. T_{m1}, T_{m2} and T_c values are gradually decreased with increase in PMDA concentration. These values were decreased approximately by 4 and 6°C, respectively, when PMDA concentration was increased to 0.3%. Compared with the T_m of virgin PET (245.4°C), RER-PET samples have similar values to virgin PET at about 0.2% PMDA concentration. Incarnato *et al.* [4] studied the chain extension process of R-PET by mixing it with high PMDA concentrations (up to 0.75%). They also re-

ported that chain extension did not significantly change T_g value while it decreased T_m, T_c, ΔH_m and ΔH_c. Lowering of T_m and T_c with increasing viscosity is indicative of effective chain extension [4, 7].

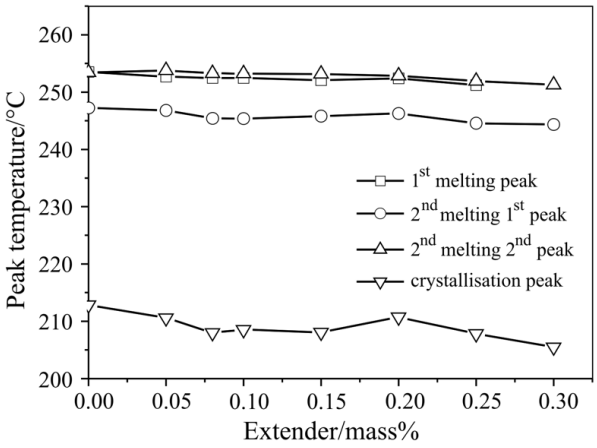

Fig. 8 Melting and crystallisation peak temperatures of RER-PET samples obtained at different PDMA content

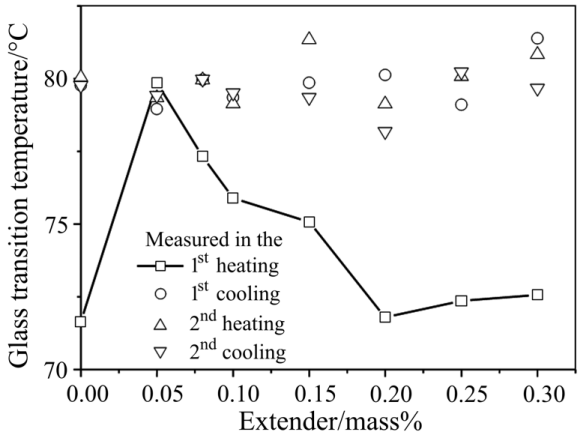

Fig. 9 Glass transition temperatures of RER-PET samples obtained at different PDMA content

Figure 9 shows the variation of T_g with the composition. T_g obtained in the first heating run shows the absence of cold crystallisation, what means that the material has partially crystallised during the preparation of the pellets after the reactive extrusion. The glass transition temperature measured in the cooling runs as well as in the second heating runs shows that the change in T_g values as a function of PDMA content is not significant. The main factor affecting the T_g of chain extended PET is the chain mobility and the degree of crystallinity. The increase in molecular mass, chain branching and

degree of cross-linking of the RER-PET is expected to increase the T_g due to the increase of the cohesive energy density [18]. However, in comparison to the T_g of virgin PET (80.5°C), RER-PET samples have similar values to the virgin PET.

TMDSC curves of chain-extended R-PET at different extruder residence times

Figure 10 shows the total heat flow curves and Fig. 11 represents the corresponding heat capacity curves of RER-PET samples obtained at different extruder residence times with 0.15 mass% PMDA concentration. The double melting peaks were clearly seen in total heat flow curves, but it appeared as a peak with a shoulder on the high temperature side in the heat capacity curves shown in Fig. 11. Again, no exothermic transitions are observed in the non-reversing heat flow curves, indicating that the double melting peaks appearing in TMDSC curves may be associated with the two different melting mechanisms. As seen before, double melting peaks were not observed for the samples with only extrusion history. The enthalpies of reversing and NR components are shown in Table 2. The scattering of the data prevents to draw any conclusion.

Figure 12 shows the total heat flow curves during first cooling runs. Again homogeneous crystallisation can be observed. There is no indication of the formation of two populations of crystals which would be the source of the double melting peak in consecutive melting.

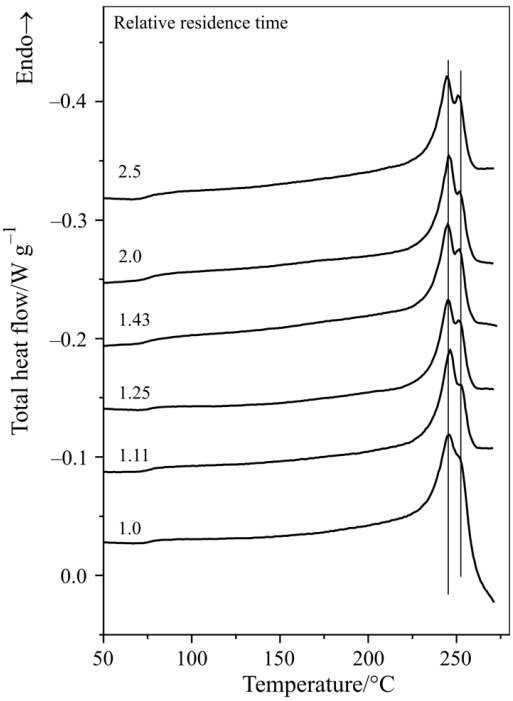

Fig. 10 TMDSC total heat flow curves of RER-PET samples obtained at constant PDMA content as a function of the relative residence time

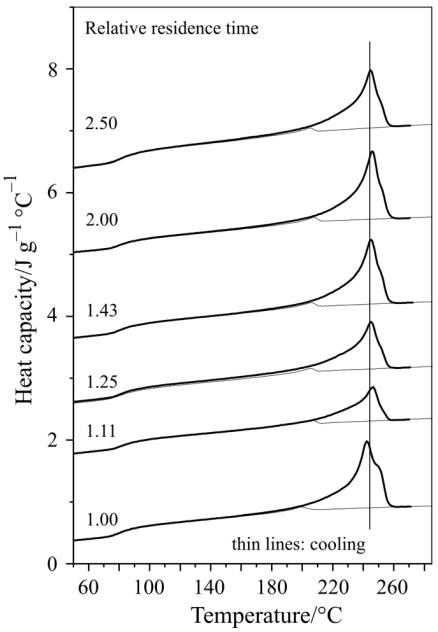

Fig. 11 TMDSC heat capacity curves of RER-PET samples obtained at different PDMA content. Recycled and virgin PET curves are included for comparison

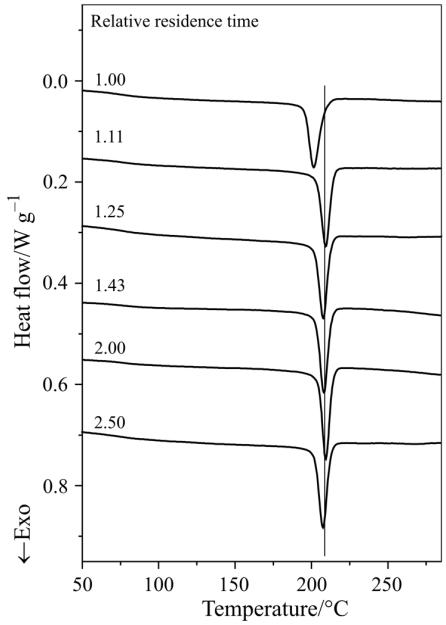

Fig. 12 TMDSC total heat flow curves of RER-PET samples obtained at constant PDMA content as a function of the relative residence time

Variations of T_g, T_m, T_c and crystallinity with extruder flow rates

Relative residence times were calculated from residence times where 1 is equal to a residence time of 45 s. The data referring to the melting enthalpies of the RER-PET samples with 0.15 mass% PDMA content as a function of the relative residence time is very much scattering, hence no conclusion can be drawn. The contributions of the reversing and non-reversing processes to the total heat of fusion are also shown in Table 2. The reaction between R-PET and PMDA is very fast, and increasing the reactive extrusion residence time could result in higher molecular mass PET with more branching and chain entanglements.

Total crystallinity gradually increases with decreasing residence time. Having more time available for PMDA molecule to react induces branching reactions with R-PET resulting in more complicated chain entanglement that depresses crystallinity. The crystallinity reduced by about 10% when the reactive extrusion process residence time was increased from the normal relative residence time of 1.0 to 2.5.

R-PET has a relatively high crystallinity value (47.7%) in comparison with virgin PET (35.5%). This is in agreement with Torres *et al.* [2] findings as the crystallinity of the R-PET sample was relatively high. The high level of crystallinity in the R-PET sample is the effect of the degradation reaction products that results from the R-PET degradation during extrusion. Degradation products, which are low molecular mass materials and short PET chains, are both relatively more mobile than the normal PET chains in the amorphous phase. The higher chain mobility i.e. lower viscosity helps the formation of the crystals. However, the effect of the degradation products is overwhelmed by the effect of high molecular mass and chain entanglements in the RER-PET samples which are introduced by PMDA chain extension. Hence for RER-PET samples a decrease in crsytallinity is observed.

Figure 13 shows the variation of the peak melting temperature and the peak temperature of the crystallisation of RER-PET samples prepared with 0.15% of PDMA

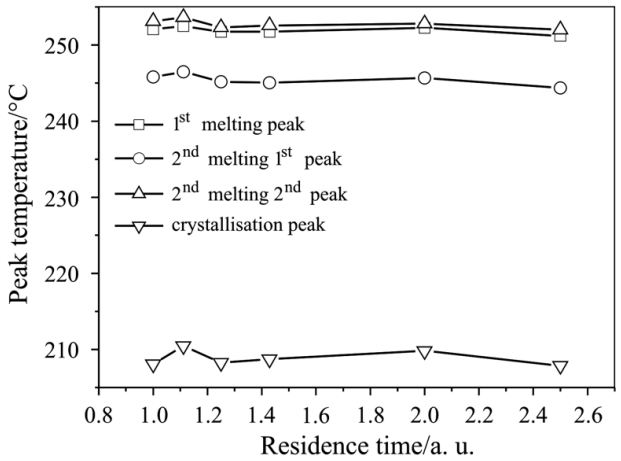

Fig. 13 Melting and crystallisation peak temperatures of RER-PET samples obtained at constant PDMA content as a function of relative residence time

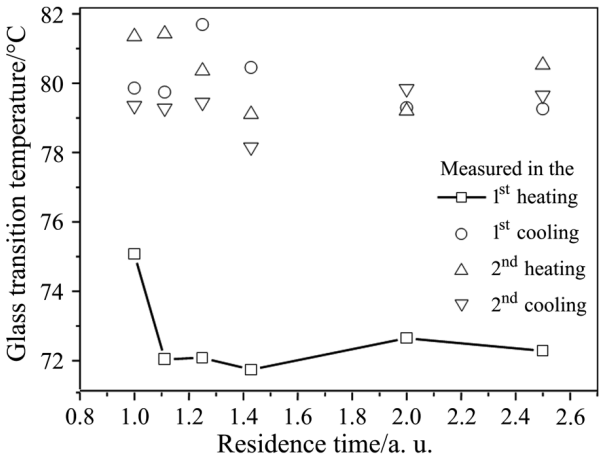

Fig. 14 Glass transition temperatures of RER-PET samples obtained at constant PDMA content as a function of the relative residence time

as a function of the relative residence time. Small decrease in the peak temperatures can be seen with increasing relative residence time.

Figure 14 shows the change of T_g as the reactive extrusion process flow rate increases. Increasing the chain extension reaction residence time slightly reduces the glass transition temperatures of the material. The data showed no significant change indicating that increasing reactive extrusion process residence time did not significantly affect the chain extension reactions of RER-PET samples. However, the T_c values remained unchanged.

Conclusions

Thermal transitions of R-PET were investigated after the chain extension process. The T_g values did not show a significant change as a function of PMDA concentration and the extrusion residence time. The T_m and T_c values decreased with increasing PMDA concentration, as well as with increasing relative residence time. Our previous work has shown that the chain extension process introduces chain branching and entanglement as demonstrated by an increase of storage moduli (G') values at a constant loss modules (G'') value with the increasing PMDA concentrations [44]. The chain branching and entanglements introduced by the chain extension process changed the RER-PET melting behaviour; two melting peaks were recorded. Total crystallinity measurements showed a small dependence on PMDA concentration in the reactive extrusion process. RER-PET crystallinity has a maximum value at a PMDA concentration of 0.25 mass%. Crystallinity also decreased with increasing chain extension reactive extrusion residence time. Thermal and crystallinity analysis confirmed that the R-PET reactive extrusion process depends more on the PMDA concentration rather than the extrusion residence time.

The first author would like to acknowledge Advanced Engineering Center for Manufacturing (AECM) and Visy Industries for their financial support to this study.

References

1 N. Cardi, R. Po, G. Giannotta, E. Occhiello, F. Garbassi and G. Messina, J. Appl. Polym. Sci., 50 (1993) 1501.
2 N. Torres, J. J. Robin and B. Bountvin, Eur. Polym. J., 36 (2000) 2075.
3 G. P. Karayannidis and E. A. Psalida, J. Appl. Polym. Sci., 77 (2000) 2206.
4 L. Incarnato, P. Scarfato, L. Di Maio and D. Acierno, Polymer, 41 (2000) 6825.
5 K. Bouma and R. J. Gaymans, Polym. Eng. Sci., 41 (2001) 466.
6 M. Xanthos, M. W. Young, G. P. Karayannidis and D. N. Bikiaris, Polym. Eng. Sci., 41 (2001) 643.
7 N. Torres, J. J. Robin and B. Bountvin, J. Appl. Polym. Sci., 79 (2001) 1816.
8 A. A. Haralabakopoulos, D. Siourvas and C. M. Paleos, J. Appl. Polym. Sci., 71 (1999) 2121.
9 D. N. Bikiaris and G. P. Karayannidis, J. Appl. Polym. Sci., 60 (1996) 55.
10 S. Japon, L. Boogh, Y. Leterrier and J. E. Manson, Polymer, 41 (2000) 5809.
11 A. J. Dijkstra, I. Goodman and J. A. W. Reid, US Patent 3 533 157 (1971)
12 Z. Bashir, I. Al-Aloush, I. Al-Raqibah and M. Ibrahim, Polym. Eng. Sci., 40 (2000) 2442.
13 H. Inata and S. Matsumura, J. Appl. Polym. Sci., 32 (1986) 4581.
14 K. C. Khemani, ANTEC Proceedings, (1998) 1934.
15 H. Al-Ghatta, S. Severini and L. Astarita, US Patent 5 422 381 (1995).
16 K. C. Khemani, C. H. Juarez-Garcia and G. D. Boone, US Patent 5 696 176 (1997)
17 H. Inata and S. Matsumura, J. Appl. Polym. Sci., 33 (1987) 3069.
18 U. W. Gedde, 'Polymer Physics' First edition, Chapman and Hall 1995.
19 S. C. Lee and B. G. Min, Polymer, 40 (1999) 5445.
20 F. J. Medellin-Rodriguez, P. J. Phillips, J. S. Lin and R. Campos, J. Polym. Sci. B, Polym. Phys., 35 (1997) 1757.
21 R. F. Rosu, R. A. Shanks and S. N. Bhattacharya, Polymer, 40 (1999) 5891.
22 F. Awaja, F. Daver and E. Kosior, Polym. Eng. Sci, Accepted for publication.
23 R.A. Shanks and F. Cser, Preprints, IUPAC MACRO'98 Gold Coast, Australia, 1998, p. 593.
24 F. Cser, J. Hopewell and R. A. Shanks, J. Therm. Anal. Cal., 54 (1998) 707.
25 F. Cser, J. L. Hopewell, K. Tajne and R.A. Shanks, J. Therm. Anal. Cal., 61 (2000) 687.
26 P. S. Gill, S. R. Sauerbrunn and M. Reading, J. Thermal Anal., 40 (1993) 931.
27 J. E. K. Schawe, Thermochim. Acta, 260 (1995) 1.
28 B. Wunderlich, A. Boller, I. Okazaki, K. Ishikiriyama, W. Chen, M. Pyda, J. Pak, I. Moon and R. Androsch, Thermochim. Acta, 330 (1999) 21.
29 S. L. Simon, Thermochim. Acta, 374 (2001) 55.
30 I. Okazaki and B. Wunderlich, Macromol. Rapid Commun.,18 (1997) 313.
31 I. Okazaki and B. Wunderlich, Macromolecules, 30 (1997) 1758.
32 C. Schick, M. Merzlyakov and B. Wunderlich, Polym. Bull., 40 (1998) 297.
33 A. Toda, C. Tomita, M. Hikosaka and Y. Saruyama, Polymer, 21 (1998) 5093.
34 D. J. Blundell and D. N. Osborne, Polymer, 24 (1983) 953.
35 F. Cser, F. Rasoul and E. Kosior, J. Thermal Anal., 50 (1997) 727.
36 M. Reading and R. J. Luyt, J. Therm. Anal. Cal., 54 (1998) 535.

37 S. Tan, A. Su, W. Li and E. Zhou, J. Polym. Sci. B, Polym. Phys., 38 (2000) 53.
38 V. B. F. Mathot, Calorimetry and Thermal Analysis of Polymers, Hanser, New York 1993, p. 232.
39 W. G. Kampert and B. B. Sauer, Polymer, 42 (2001) 8703.
40 B. Wunderlich, A. Boller, I. Okazaki and A. Kreitmeier, Thermochim. Acta, 282/283 (1996) 143.
41 Z. Yuan, R. Song and D. Shen, Polym. Int., 49 (2000) 1377.
42 J. J. Janimark and G. C. Stevens, Thermochim. Acta, 332 (1999) 125.
43 M. Jollands, F. Cser and A. Chryss, ANTEC 2002, SPE, San Francisco, Preprints Paper #: 848 (2002).
44 F. Daver, R. Gupta and E. Kosior, PPS-2003, Vouliagmeni, Greece, Paper#154 (2003).